Impact of downwind sampling location and height on inverse-Gaussian dispersion modeling: A theoretical study

Heather W Jones, Lingjuan Wang-Li[*], Behdad Yazdani Boroujeni

(*Department of Biological and Agricultural Engineering*, *North Carolina State University*, *Raleigh*, *NC 27695-7625 USA*)

Abstract: In the studies of fate and transport of air emissions from animal feeding operations, Gaussian based dispersion models have been commonly used to predict downwind pollutant concentrations through forward modeling approach, or to derive emission rates and emission factors through inverse dispersion modeling approach. In the Gaussian dispersion modeling process, downwind sampling location and sampling height could generate significant impact on accuracy of the model validation, or inverse modeling results based upon field measurements. This study theoretically analyzed the impact of downwind locations and sampling height on Gaussian dispersion modeling. It was discovered that the field sampling needs to be conducted at the locations beyond the plume touching-ground distance, at a downwind distance as short as 5 m for the case scenario with zero rise of emission plume under the atmospheric stability class C, or as long as 297 m for the case scenario with 15 m rise of emission plume under the atmospheric stability class F. In order to measure the PM concentrations of the dispersion plume, the minimum sampling height at the locations within the plume touching-ground distance varied from ground level to as high as almost 14 m, whereas for the locations beyond the plume touching-ground distance, a sampling height of ground level would be acceptable.

Keywords: animal feeding operations, Gaussian dispersion modeling, downwind distance, downwind sampling location, downwind sampling height

1　Introduction

Air emissions from animal housing systems are of increasing interest due to the magnitude of the emissions and their adverse health and environmental effects on local communities[1-3]. In evaluation of environmental

Biographies: Heather W Jones, undergraduate research assistant, Department of Mathematics, Meredith College, Raleigh, NC 27607 & Department of Civil, Constuction and Enviromental Engineering, North Carolina State University, Raleigh, NC27695. Email: joneshw@email.meredith.edu. **Behdad Yazdani Boroujeni**, Department of Civil, Constuction and Enviromental Engineering, North Carolina State University, Raleigh, NC27695. Email: byazdan@ncsu.edu.
*Corresponding author: Lingjuan Wang-Li, Associate Professor, Department of Biological and Agricultural Engineering, North Carolina State University. 186 Weaver Labs, Campus Box 7625, NCSU, Raleigh, NC 27695-7625. Tel: (919) 515-6762; Fax: (919) 515-7760; Email: Lwang5@ncsu.edu; ling_wang@ncsu.edu.

and health impacts of air emissions of a given source, knowledge about the emission generation, fate and transport is required. While quantifying and modeling generations of air emissions from animal feeding operations (AFOs) have been the subjects of numerous research projects for decades[3], limited studies have been conducted on estimating and modeling the fate and transport of air emissions from AFO facilities[4-9]. In the studies of fate and transport of the AFO air emissions, Gaussian based dispersion models have been commonly used to predict downwind pollutant concentrations through forward modeling approach, or to derive emission rates and emission factors through inverse dispersion modeling approach. In these dispersion modeling processes, field measurements of downwind pollutant concentrations were usually taken in conjunction with ambient meteorological conditions for validation of forward modeling results when the emission

rate was known, or for inverse modeling calculations of the emission rates when the emission rate was unknown.

Among various Gaussian based models, AERMOD-PRIME is one type of computer program used by the United State Environmental Protection Agency (US EPA) to estimate dispersions of the pollutants from various sources, i.e. point, line, and area sources. Faulkner et al.[9] conducted a study to estimate the impact of particulate matter (PM) sampler placement on inverse AERMOD results for ground level area source PM emission factor determination. It was reported that the field sampler placement has significant impact on accuracy of the modeling results. To reduce uncertainty associated with inverse modeling results (the emission fluxes) from field measured downwind concentrations, the field samplers should be placed close to the resource and along the line of maximum concentration to minimize edge effect of the area source.

Hensen et al.[8] used a Gaussian-3D plume model as well as the Huang-3D model to estimate emissions. Both of the models use the general superposition principle to relate the concentration at one location to the source strength at a different location by using a dispersion function. Each model has different ways in calculating this dispersion function. The Gaussian-3D model utilizes constant wind speed and diffusivity profile while the wind speed increases with height in the Huang-3D model, thus resulting in differences in final calculations[8]. Both of these models are found to be affected by surface roughness (smooth or rough), height and size of the source, and atmospheric stability classes, much like the Gaussian dispersion model used in this study.

As reported by Cooper and Alley[10], the fundamental Gaussian dispersion equation takes the following form:

$$C = \frac{Q}{2\pi U \sigma_y \sigma_z} \exp\left(-\frac{1}{2}\frac{y^2}{\sigma_y^2}\right)\left\{\exp\left(-\frac{1}{2}\frac{(z-H)^2}{\sigma_z^2}\right) + \exp\left(-\frac{1}{2}\frac{(z+H)^2}{\sigma_z^2}\right)\right\} \quad (1)$$

where, C (μg/m^3) = steady-state concentration at a point (x, y, z); Q (μg/s) = emissions rate; σ_y, σ_z (m) = horizontal and vertical spread parameters, respectively; U (m/s) =

average wind speed at stack height; y (m) = horizontal distance from plume centerline; z (m) = vertical distance from ground level; H (m) = effective stack height ($H = h + \Delta h$, with h = physical stack height and Δh = plume rise).

In this equation, an imagery reflective source term was added to account for the fact that pollutants cannot disperse underground, shown in Figure 1[10], while it is necessary to include an imaginary reflective term at the locations beyond the plume touching-ground location. Inclusion of the reflection may cause significant errors in model prediction and validation at the downwind locations within the distance from the source to the location where the plume touches the ground.
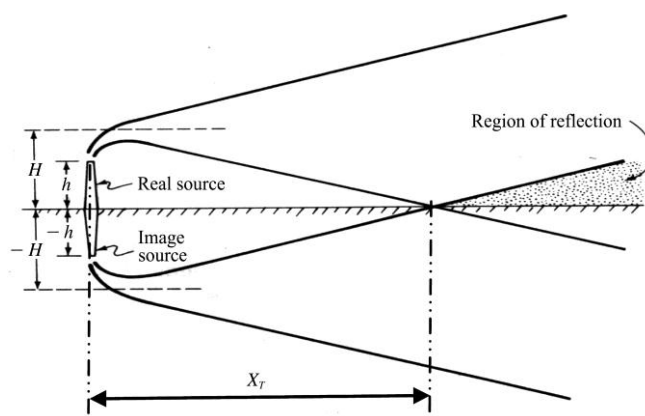

Figure 1   Illustration of the imaginary reflective source term in Gaussian dispersion model and the plume touching-ground distance (X_T)[10]

In addition to the impact of downwind location, the field sampling height will also generate significant impact on the accuracy of the model validation, or inverse modeling results based upon field measurements. If an air sampler is placed at a height below the bottom edge of the plume, measurements of the sampler will not represent downwind plume concentrations. It is important that the vertical plume spread parameter (σ_z) needs to be taken into account in determination of downwind sampling distance and downwind sampling height. This paper reports a theoretical study of impact of downwind sampler placement (location and the sampling height) on accuracy of the model validation or results of the inverse Gaussian dispersion modeling based upon field measurements.

2   Methodology

2.1   Case scenarios

For this theoretical study, PM emission from an animal housing ventilation system was used as an example to investigate Gaussian dispersion model predictions of downwind concentrations under different case scenarios.   As shown in Figure 2, although the emission "stack" of the housing ventilation fans was near the ground level (1.5 m above the ground), the exhaust plume may reach the top of the background trees (14 m high).   The plume-rise of the air emissions from this animal housing system was caused by velocity momentum of the exhaust fans and the thermal lifting of the exhaust air due to temperature difference between emitted air and surrounding air.   Thus, the plume-rise of air emission from animal housing system is a function of the exhaust ventilation fan flow rate and the temperature difference between the exhaust air and the ambient air. Consequently, the plume rise varies over different seasons and under different ventilation settings.

Figure 2   Air emission plume from a tunnel ventilated poultry house

Based upon the field observations, a group of assumptions were made for conducting this theoretical study (shown in Table 1).   In addition, the analysis was focused on the plume centerline, therefore the horizontal distance from the plume centerline, y, is zero.

Table 1   Case scenarios for the theoretical analysis in this study

Parameters	Assumptions
PM$_{10}$ emission rate, Q	10^6 µg s^{-1}
Physical stack height, h	1.5 m
Plume-rise, Δh	0, 3, 5, 10, and 15 m
Wind speed at 10 m above the ground, U_{10}	1, 3, 5, and 15 m s^{-1}
PM$_{10}$ sampler/monitor height, Z	1.5 m
Atmospheric stability classes	A, B, C, D, E, F

In application of Gaussian model to predict downwind PM concentrations, building downwash and PM settling are also important factors that need to be considered.   The theoretical analysis of this reported study aimed to examine the impacts of downwind sampling location in response to the imaginary reflective term in Gaussian model and the sampling heights in response to the plume width (bottom edge) under different atmospheric conditions.   This study does not include the building downwash and PM settling in analysis, so extreme cautions need to be taken when interpolating the results to the case scenarios where building downwash and PM settling (especially for large particles) become a significant concern.

2.2   Gaussian dispersion modeling: with vs. without imaginary reflective source term

In order to estimate impact of downwind location on the accuracy of Gaussian dispersion modeling, PM$_{10}$ concentrations at different downwind distances for different case scenarios were calculated using two Gaussian equations, in which one includes the imaginary reflective source term (Equation (2)) and the other one does not include the reflective term (Equation (3)). Equations (2) and (3) are Gaussian models for calculations of downwind PM$_{10}$ concentrations on the plume centerline with (C_w) and without ($C_{w/o}$) reflective source term, respectively.   Definitions of the parameters in these two equations are the same as those in Equation (1).

$$C_w = \frac{Q}{2\rho U S_y S_z} \left\{ \exp\left[-\frac{1}{2} \frac{(z-H)^2}{S_z^2} \right] + \exp\left[-\frac{1}{2} \frac{(z+H)^2}{S_z^2} \right] \right\}$$
(2)

$$C_{w/o} = \frac{Q}{2\rho U S_y S_z} \exp\left[-\frac{1}{2} \frac{(z-H)^2}{S_z^2} \right]$$
(3)

2.2.1   Wind speed at stack height determination

In Equations (2) and (3), wind speed (U) was defined at the stack height.   Consequently, wind speed at 10 m above the ground needs to be converted to the stack height.   The wind profile power law was used to do the wind speed conversion[10]:

$$U = U_{10} \left(\frac{Z_2}{Z_1} \right)^p$$
(4)

where, U = wind speed at the stack height; U_{10} = wind speed at 10 m above the ground; Z_1 = elevation 1, or 10 m for this study; Z_2 = elevation 2, or physical stack height, h = 1.5 m, for this study; p = exponent.

The exponent p is dependent upon atmospheric stability classes as well as the type of surface that the emission source is located on.   Since the animal housing system considered in this study is located in a rural region, smooth surface is used when finding U.   The exponent p was determined using Table 2.

Table 2   Exponents for wind profile power law model (Equation (4)) [*]

Stability class [**]	Exponent (p)	
	Rough surface (urban)	Smooth surface (rural)
A	0.15	0.07
B	0.15	0.07
C	0.20	0.10
D	0.25	0.15
E	0.30	0.35
F	0.30	0.35

Note: [*]Adapted from Cooper and Alley[10]. [**]Atmospheric turbulence is categorized into six stability classes named A, B, C, D, E and F, with class A being the most unstable or most turbulent class, and class F being the most stable or least turbulent class.

2.2.2   Plume spread parameters (σ_y, σ_z)

The horizontal and vertical spread parameters, σ_y (m) and σ_z (m), are functions of atmospheric stability; along with downwind distance X (km), are defined as the following[10]:

$$\sigma_y = aX^b \tag{5}$$
$$\sigma_z = cX^d + f \tag{6}$$

where, a, b, c, d, and f are constants that are dependent upon stability class and downwind distance.   These constants can be determined from Table 3.

Table 3   Values for constants used in spread parameters equations[*]

Stability	a	b	$X < 1$ km			$X > 1$ km		
			c	d	f	c	d	f
A	213	0.894	440.8	1.941	9.27	459.7	2.094	-9.6
B	156	0.894	106.6	1.149	3.3	108.2	1.098	2.0
C	104	0.894	61.0	0.911	0	61.0	0.911	0
D	68	0.894	33.2	0.725	-1.7	44.5	0.516	-13.0
E	50.5	0.894	22.8	0.678	-1.3	55.4	0.305	-34.0
F	34	0.894	14.35	0.740	-0.35	62.6	0.180	-48.6

Note: [*]Adapted from Cooper and Alley[10].

2.3   Determination of the plume touching-ground distances

Since the plume touching-ground location is a threshold where the imaginary reflective source term should be considered in the model prediction, the first step of this study was to calculate this critical location.   As it is well known that when the plume edge is defined as three standard deviations away from the centerline ($3\sigma_z$), the plume contains 99.74% of the total mass of the plume, where the edge concentration is only 1.1% of the centerline concentration (peak value)[10].   Thus, in this theoretical study, the $3\sigma_z$ was defined as the half plume width.   Consequently, at the plume touching-ground downwind distance, the effective stack height (H) equals the half of the plume width, i.e. $3\sigma_z$ (Figure 3).   The touching-ground distance could be determined by setting $3\sigma_z$ equal to H in Equation (6).   Equation (6) can then be rewritten to solve for X_T as following:

$$X_T = \left(\frac{H - 3f}{3c} \right)^{1/d} \tag{7}$$

where, c, d, and f are determined from Table 3.   It is important to notice that in this table, there are two columns of numbers to choose from, one for $X < 1$ km and one for $X > 1$ km.   This must be considered for each downwind distance, X, and the values for c, d, and f must be chosen accordingly.

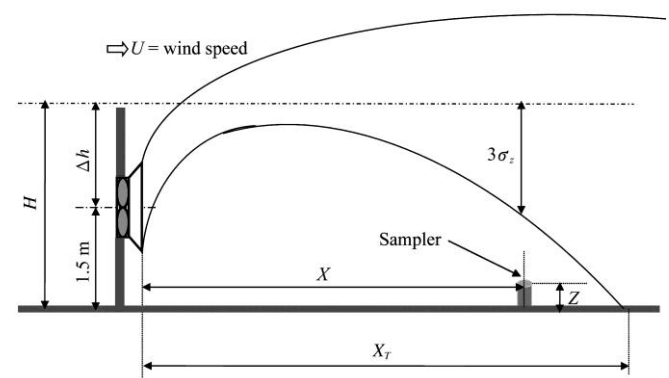Figure 3   Illustration of the plume from a ventilation fan and the plume touching-ground distance (X_T)

This study focuses on downwind distances where $X < X_T$, $X = X_T$, and $X > X_T$.   The downwind distance values chosen were ¼ X_T, ½ X_T, ¾ X_T, X_T, 1.5 X_T, and   2 X_T.   These downwind distances were calculated for each effective stack height, and these values were then used in

Equations (5) and (6) to determine the horizontal and vertical spread parameters at each effective stack height.

2.4   Comparisons of the modeling results

As shown in Table 1, numerous scenarios were considered in this study.   A combination of downwind distances, vertical distances from ground level, effective stack height (physical stack height plus plume rise), and wind speed at the stack height were considered for every stability class.   Once all scenarios possible were determined, Equations (2) and (3) were used to determine the steady-state concentrations including and excluding the reflection term.

To compare the modeling results including or excluding the reflective term, a relative difference (*RD*, %) term was introduced and computed using Equation (8).

$$RD = \left[\frac{C_w - C_{w/o}}{C_{w/o}} \right] * 100 \qquad (8)$$

2.5   Determination of the minimum sampling heights at various downwind distances

As shown in Figure 3, when the sampling height *Z* is smaller than the effective stack height *H* minus the half of the vertical plume width ($3\sigma_z$), the sampling height is below the plume bottom edge.   Consequently, the sampler would not be placed within the plume in order to validate the Gaussian dispersion model.   It is recommended that in the Gaussian dispersion modeling study, the minimum sampling height for downwind plume measurements is at the bottom edge of the plume, i.e. $H-3\sigma_z$.

3   Results and discussion

3.1   Plume touching-ground distances

The plume touching-ground distances under different conditions were calculated using Equation (7) (Table 4).   As it is observed, higher plume rise causes longer plume touching-ground distance, and unstable atmospheric condition causes shorter touching-ground distance.

3.2   Comparison of the Gaussian model predictions: with vs. without reflective source term

Based upon the defined scenarios listed in Table 1, Equations (2) and (3) were used to determine the steady-state downwind PM concentrations including and excluding the reflective source term.   Tables 5-8

Table 4   Calculated touching-ground distances (X_T, m) under different conditions

Stability class	Plume rise (Δh)				
	0 m	3 m	5 m	10 m	15 m
A	-*	-	-	-	-
B	-	-	-	10	34
C	5	17	26	48	71
D	24	40	52	84	121
E	24	45	62	111	168
F	22	63	95	189	297

Note: *No valid result was obtained for the given case scenario.

compared the downwind mean concentrations calculated by the models including and excluding the reflective source term (Equations (2) and (3)) at different downwind locations and under different wind speeds and plume rises. The mean concentration for any given condition (combination of wind speed, plume rise and downwind location) is the average concentration for the stability classes A-F.

As shown in Tables 5-8, at the zero and low plume rises (Δh equals 0, 3, and 5 m), there was no significant difference among downwind mean concentrations predicted by models including and excluding the reflective source term for downwind distance within the plume touching-ground point.   However, as the plume rise increased, the differences in downwind mean concentration predictions by models including and excluding reflective terms increased.   Also, at the lower wind speed, the higher differences in means model predictions was observed.   For the high plume-rise (Δh equals 10 and 15 m) and the downwind locations within the plume touching-ground distance, inclusion of the reflective source term increased downwind concentration predictions, thus caused over predictions of the downwind concentrations.   This observation indicates that when a field sampling is conducted for validating Gaussian models, or for conducting inverse modeling to derive emission rate from a given source, either the sampling/measurements need to be conducted at the locations beyond the plume touching-ground distance, or the reflective source term needs to be excluded in the model if the sampling location is within the plume touching-ground distance.   Based upon the touching-ground distance listed in Table 4, it is recommended that

in application of conducting Gaussian dispersion modeling, the field sampler should be placed at a downwind distance as short as 5 m for the case scenario with zero plume rise and atmospheric stability class C, or as long as 297 m for the case scenario with 15 m plume rise and atmospheric stability class F.

Table 5   Comparisons of the predicted concentrations at different downwind distances for U_{10}=1 m s^{-1}

Downwind location	Δh=0 m		Δh=3 m		Δh=5 m		Δh=10 m		Δh=15 m	
	C_w (µg m^{-3})	$C_{w/o}$ (µg m^{-3})	C_w (µg m^{-3})	$C_{w/o}$ (µg m^{-3})	C_w (µg m^{-3})	$C_{w/o}$ (µg m^{-3})	C_w (µg m^{-3})	$C_{w/o}$ (µg m^{-3})	C_w (µg m^{-3})	$C_{w/o}$ (µg m^{-3})
¼ X_T	-	-	1.42E-14	1.42E-14	7.32E-13	7.32E-13	3.45E+02	3.28E+02	2.50E+00	2.43E+00
½ X_T	3.23E+06	3.23E+06	5.22E+01	5.22E+01	5.26E+00	5.26E+00	2.48E+02	2.33E+02	8.27E+00	7.75E+00
¾ X_T	1.15E+06	1.15E+06	2.69E+03	2.69E+03	5.20E+02	5.19E+02	2.72E+02	2.54E+02	3.64E+01	3.30E+01
X_T	5.12E+05	4.51E+05	8.29E+04	5.48E+04	4.14E+04	2.54E+04	1.64E+04	9.29E+03	5.95E+03	3.24E+03
1.5 X_T	1.78E+05	1.77E+05	1.40E+04	1.30E+04	5.29E+03	4.63E+03	1.09E+03	2.04E+03	4.50E+02	3.20E+02
2 X_T	1.05E+05	9.92E+04	1.34E+04	1.11E+04	5.96E+03	4.57E+03	1.38E+03	9.88E+02	6.33E+02	4.07E+02

Table 6   Comparisons of the predicted concentrations at different downwind distances for U_{10}=3 m s^{-1}

Downwind location	Δh=0 m		Δh=3 m		Δh=5 m		Δh=10 m		Δh=15 m	
	C_w (µg m^{-3})	$C_{w/o}$ (µg m^{-3})	C_w (µg m^{-3})	$C_{w/o}$ (µg m^{-3})	C_w (µg m^{-3})	$C_{w/o}$ (µg m^{-3})	C_w (µg m^{-3})	$C_{w/o}$ (µg m^{-3})	C_w (µg m^{-3})	$C_{w/o}$ (µg m^{-3})
¼ X_T	1.68E+06	1.68E+06	1.32E-06	1.32E-06	1.61E-10	1.61E-10	8.62E+01	8.20E+01	6.26E-01	6.08E-01
½ X_T	7.79E+05	7.79E+05	2.70E+01	2.70E+01	1.88E+00	1.88E+00	6.20E+01	5.83E+01	2.07E+00	1.94E+00
¾ X_T	3.33E+05	3.33E+05	8.97E+02	8.97E+02	1.63E+02	1.62E+02	7.13E+01	6.69E+01	1.01E+01	9.19E+00
X_T	1.66E+05	1.46E+05	2.47E+04	1.63E+04	1.22E+04	7.51E+03	4.85E+03	2.74E+03	1.85E+03	1.01E+03
1.5 X_T	6.17E+04	6.15E+04	4.12E+03	3.86E+03	1.56E+03	1.37E+03	3.49E+02	2.74E+02	1.48E+02	1.04E+02
2 X_T	3.66E+04	3.52E+04	3.99E+03	3.31E+03	1.77E+03	1.35E+03	4.47E+02	3.13E+02	2.07E+02	1.32E+02

Table 7   Comparisons of the predicted concentrations at different downwind distances for U_{10}=5 m s^{-1}

Downwind location	Δh=0 m		Δh=3 m		Δh=5 m		Δh=10 m		Δh=15 m	
	C_w (µg m^{-3})	$C_{w/o}$ (µg m^{-3})	C_w (µg m^{-3})	$C_{w/o}$ (µg m^{-3})	C_w (µg m^{-3})	$C_{w/o}$ (µg m^{-3})	C_w (µg m^{-3})	$C_{w/o}$ (µg m^{-3})	C_w (µg m^{-3})	$C_{w/o}$ (µg m^{-3})
¼ X_T	1.01E+06	1.01E+06	1.58E-06	1.58E-06	1.93E-10	1.93E-10	5.17E+01	4.92E+01	3.75E-01	3.65E-01
½ X_T	2.88E+05	2.88E+05	9.26E+00	9.26E+00	4.30E-01	4.30E-01	3.72E+01	3.49E+01	1.23E+00	1.15E+00
¾ X_T	2.18E+05	2.18E+05	2.95E+02	2.95E+02	5.73E+01	5.73E+01	4.00E+01	3.75E+01	5.33E+00	4.85E+00
X_T	7.10E+04	6.25E+04	1.20E+04	7.94E+03	6.21E+03	3.81E+03	2.72E+03	1.54E+03	1.04E+03	5.66E+02
1.5 X_T	2.44E+04	2.41E+04	2.13E+03	1.95E+03	8.57E+02	7.36E+02	4.15E+02	3.47E+02	8.64E+01	6.05E+01
2 X_T	1.47E+04	1.35E+04	2.02E+03	1.67E+03	9.50E+02	7.04E+02	4.78E+02	3.50E+02	1.20E+02	7.56E+01

Table 8   Comparisons of the predicted concentrations at different downwind distances for U_{10}=15 m s^{-1}

Downwind location	Δh=0 m		Δh=3 m		Δh=5 m		Δh=10 m		Δh=15 m	
	C_w (µg m^{-3})	$C_{w/o}$ (µg m^{-3})	C_w (µg m^{-3})	$C_{w/o}$ (µg m^{-3})	C_w (µg m^{-3})	$C_{w/o}$ (µg m^{-3})	C_w (µg m^{-3})	$C_{w/o}$ (µg m^{-3})	C_w (µg m^{-3})	$C_{w/o}$ (µg m^{-3})
¼ X_T	3.36E+05	3.36E+05	5.28E-07	5.28E-07	6.43E-11	6.43E-11	9.97E-16	9.97E-16	9.34E-18	9.34E-18
½ X_T	9.61E+04	9.61E+04	4.63E+00	4.63E+00	2.14E-01	2.14E-01	1.28E-02	1.28E-02	8.68E-04	8.65E-04
¾ X_T	6.75E+04	6.75E+04	9.95E+01	9.95E+01	1.73E+01	1.72E+01	1.08E+01	1.06E+01	7.19E-01	6.79E-01
X_T	2.23E+04	1.96E+04	3.39E+03	2.24E+03	1.74E+03	1.06E+03	2.60E+03	1.47E+03	2.95E+02	1.61E+02
1.5 X_T	8.35E+03	8.26E+03	5.94E+02	5.44E+02	2.42E+02	2.06E+02	2.58E+02	1.96E+02	2.89E+01	1.98E+01
2 X_T	5.03E+03	4.76E+03	5.65E+02	4.50E+02	2.68E+02	1.97E+02	1.72E+02	2.26E+02	3.92E+01	2.41E+01

To further investigate the impact of downwind location on the modeling results including or excluding the reflective term, the relative difference (RD) was calculated using Equation (8). Table 9 lists mean RDs for the stability classes A-F under different scenarios (combination of different wind speeds, plume rises, and downwind distances). As it can be seen, the RD increases with increase of the plume rise. At the downwind locations within the plume touching-ground distance ($X < X_T$), the RD may reach close to 9% at the

downwind distance of ¾ X_T when wind speed was 1 m/s and the plume rise was 15 m. This RD may cause errors in the forward or inverse Gaussian model predictions if the reflective source term was not excluded. The alternative way to minimize the error caused by the reflective source term is to place the sampler beyond the touching-ground distances.

Table 9   Summary of the RDs (%) defined in Equation (8)

Downwind location	Δh=0 m	Δh=3 m	Δh=5 m	Δh=10 m	Δh=15 m
			U_{10}=1 m s⁻¹		
¼ X_T	-*	0.00E+00	0.00E+00	1.71E+00	9.82E-01
½ X_T	0.00E+00	3.06E-09	2.35E-05	2.15E+00	2.61E+00
¾ X_T	0.00E+00	1.77E-03	6.69E-02	3.99E+00	8.97E+00
X_T	1.35E+01	5.13E+01	6.30E+01	7.70E+01	8.34E+01
1.5 X_T	1.02E+00	7.34E+00	1.41E+01	1.90E+01	3.97E+01
2 X_T	9.22E+00	2.14E+01	3.04E+01	3.74E+01	5.44E+01
			U_{10}=3 m s⁻¹		
¼ X_T	0.00E+00	0.00E+00	0.00E+00	1.28E+00	7.36E-01
½ X_T	0.00E+00	2.24E-08	2.96E-05	1.62E+00	2.04E+00
¾ X_T	2.09E-12	1.27E-02	7.45E-02	3.47E+00	8.30E+00
X_T	1.35E+01	5.13E+01	6.30E+01	7.70E+01	8.34E+01
1.5 X_T	6.87E-01	2.21E+01	1.40E+01	2.67E+01	4.12E+01
2 X_T	6.35E+00	2.04E+01	3.06E+01	4.09E+01	5.66E+01
			U_{10}=5 m s⁻¹		
¼ X_T	0.00E+00	0.00E+00	0.00E+00	1.28E+00	7.36E-01
½ X_T	0.00E+00	2.04E-08	1.39E-05	1.60E+00	1.89E+00
¾ X_T	2.08E-12	1.38E-03	4.28E-02	3.18E+00	7.82E+00
X_T	1.35E+01	5.13E+01	6.30E+01	7.70E+01	8.34E+01
1.5 X_T	2.55E+00	9.49E+00	1.66E+01	2.42E+01	4.22E+01
2 X_T	1.57E+01	3.08E+01	3.53E+01	3.93E+01	5.78E+01
			U_{10}=15 m s⁻¹		
¼ X_T	0.00E+00	0.00E+00	0.00E+00	8.96E-12	6.53E-08
½ X_T	0.00E+00	3.06E-08	2.09E-05	1.63E-02	1.98E-01
¾ X_T	3.13E-12	1.99E-03	4.89E-02	1.83E+00	5.95E+00
X_T	1.35E+01	5.13E+01	6.30E+01	7.70E+01	8.34E+01
1.5 X_T	2.84E+00	9.57E+00	1.69E+01	3.20E+01	4.58E+01
2 X_T	1.54E+01	2.67E+01	3.61E+01	5.00E+01	6.25E+01

Note: *No valid result was obtained in this case scenario.

Since the reflective source term was added into Gaussian model to account for the fact that pollutants cannot disperse underground, excluding this term at the locations beyond the plume touching-ground would also cause some errors in modeling results. Tables 5-9 show the errors caused by excluding the reflective term at locations of X_T, 1.5 X_T, and 2 X_T. Since by default, the reflective term is included in the Gaussian models, this type of error usually should not be a concern.

3.3   Minimum sampling heights

For field study of Gaussian dispersion modeling, the minimum sampling height should be at the height of the bottom edge of the plume, which is the effective stack height minus the half of the vertical plume width. The height of the plume bottom edge changes with the change of downwind distance, therefore the minimum sampling height also changes. Table 10 summarizes the minimum sampling heights under different plume rises, stability classes and downwind distances. As it can be seen, the minimum sampling height at the locations within the plume touching-ground distance varied from ground level near to as high as 14 m, whereas for the locations beyond the plume touching-ground distance, any ground level sampling height would be acceptable. In field study of Gaussian dispersion modeling, the minimum sampling height needs to be taken into considerations based upon downwind distance, plume rise and meteorological conditions.

Table 10   Calculated minimum sampling heights (H-3σ_z, m) under different plume-rises (Δh), stability classes (A-F), and downwind distances

Downwind location	A	B	C	D	E	F
			Δh=0 m			
¼ X_T	-*	-	1.08	-	-	-
½ X_T	-	-	0.70	-	-	1.02
¾ X_T	-	-	0.35	1.24	0.96	0.49
			Δh=3 m			
¼ X_T	-	-	3.23	-	-	3.56
½ X_T	-	-	2.11	3.79	3.15	2.23
¾ X_T	-	-	1.04	1.81	1.49	1.06
			Δh=5 m			
¼ X_T	-	-	4.66	-	6.34	4.84
½ X_T	-	-	3.04	4.58	3.90	3.03
¾ X_T	-	-	1.50	2.18	1.84	1.45
			Δh=10 m			
¼ X_T	-	1.27	8.25	10.52	9.38	8.05
½ X_T	-	0.88	5.38	6.56	5.77	5.04
¾ X_T	-	0.45	2.65	3.13	2.73	2.41
			Δh=15 m			
¼ X_T	-	5.26	11.83	13.69	12.43	11.26
½ X_T	-	3.62	7.73	8.53	7.65	7.04
¾ X_T	-	1.86	3.80	4.07	3.61	3.37

Note: *No valid result was obtained in this case scenario.

4   Conclusions

This theoretical study investigated the impact of the reflective source term in Gaussian model on downwind PM_{10} concentration predictions at different distances and under different meteorological conditions and plume rises. This impact may transfer to the impact of downwind locations on Gaussian dispersion modeling results. It was discovered that for the downwind locations within the plume touching-ground distance, inclusion of the reflective source term significantly increased downwind concentration predictions for emission source with plume-rise at 10 m or above, thus caused over predictions of the downwind concentrations. This observation indicates that when a field sampling is conducted for validating Gaussian models, or for conducting inverse modeling to derive emission rate from a given source, the field sampling needs to be conducted at the locations beyond the plume touching-ground distance. It is recommended that in application of conducting Gaussian dispersion modeling study, the field sampler should be placed at a downwind distance as short as 5 m for the case scenario with zero plume rise and atmospheric stability class C, or as long as 297 m for the case scenario with 15 m plume rise and atmospheric stability class F.

In addition to the sampler placement at the downwind locations, in field study of Gaussian dispersion modeling, the minimum sampling height needs to be taken into consideration such that the samplers may reach the bottom edge of the plume. It was discovered that the minimum sampling height at the locations within the plume touching-ground distance varied from ground level to as high as close to 14 m, whereas for the locations beyond the plume touching-ground distance, any ground level sampling height would be acceptable.

While this theoretical study provides much needed information about the impacts of downwind sampling location and sampling height on the accuracy of inverse-Gaussian dispersion modelling, it is realized that the theoretical study may not be sufficient to fully address all the sceneries in real-world situations. Experimental investigation is recommended to verify the findings of this study.

Acknowledgements

[References]

[1]   EPA. Ohio's largest egg producer agrees to dramatic air pollution reductions from three giant facilities. Environmental Protection Agency. Release date: Feb. 23, 2014. Available at http://yosemite.epa.gov/opa/admpress.nsf/b1ab9f485b098972852562e7004dc686/508199b8068c24a585256e43007e1230!OpenDocument.

[2]   EPA. Air Quality Compliance Agreement for Animal Feeding Operations. 2005. Available at http://www.epa.gov/compliance/resources/agreements/caa/cafo-agr-0501.html. Access on July 14, 2011.

[3]   National Research Council. Air emissions from animal feeding operations: Current knowledge, future needs. The National Academies Press, Washington DC, 2003.

[4]   O'Shaughnessy P T, Altmaier R. Use of AERMOD to determine a hydrogen sulfide emission factor for swine operations by inverse modeling. Atmospheric Enviornment, 2011; 45(27): 4617-4625.

[5]   Hoff S J, Bundy D S, Harmon J D. Modeling receptor odor exposure from swine production sources using CAM. Applied Engineering in Agriculture, 2008; 24: 821-837.

[6]   Guo H, Jacobson L D, Schmidt D R, Nicolai R E, Janni K A. Comparison of five models for setback distance determination from livestock sites. Canadian Biosystems Engineering, 2004; 46: 6.17-6.25.

[7]   Flesch T K, Harper L A, Powell J M, Wilson J D. Inverse dispersion calculation of ammonia emissions from Wisconsin dairy farms. Transactions of the ASABE, 2009; 52: 253-265.

[8]   Hensen A, Loubet B, Mosquera J, van den Bulk W C M, Erisman J W, Dämmgen U, et al. Estimation of NH_3 emissions from a naturally ventilated livestock farm using local-scale atmospheric dispersion modeling. Biogeosciences Discussions, 2009; 6: 2847-2860.

[9]   Faulkner W B, Lange J M, Powell J J, Shaw B W, Parnell C B. Sampler placement to determine emission factors from ground level area sources. Paper No. 074103, 2007 ASABE annual international meeting. Minneapolis, Minnesota, June 17-20, 2007.

[10] Cooper C D, Alley F C. Air pollution control: A design approach. Waveland Press, Prospect Heights, Ill. 2002.